

A geometric description of nonreciprocity in coupled two-mode systems

This content has been downloaded from IOPscience. Please scroll down to see the full text.

2014 New J. Phys. 16 103027

(<http://iopscience.iop.org/1367-2630/16/10/103027>)

View [the table of contents for this issue](#), or go to the [journal homepage](#) for more

Download details:

IP Address: 132.163.53.155

This content was downloaded on 27/11/2015 at 17:50

Please note that [terms and conditions apply](#).

A geometric description of nonreciprocity in coupled two-mode systems

Leonardo Ranzani and José Aumentado

National Institute of Standards and Technology, Boulder, CO 80305, USA

E-mail: leonardo.ranzani@colorado.edu and jose.aumentado@nist.gov

Received 10 July 2014, revised 20 August 2014

Accepted for publication 1 September 2014

Published 16 October 2014

New Journal of Physics **16** (2014) 103027

doi:[10.1088/1367-2630/16/10/103027](https://doi.org/10.1088/1367-2630/16/10/103027)

Abstract

We explore the concept of nonreciprocity in coupled two-mode systems using a geometric mapping to the Poincaré sphere. From this perspective, we recast the requirements for nonreciprocity in terms of rotation and inversion symmetry arguments for the vector describing the two-mode state. We provide a few examples (the microwave circulator, parametric up/down converter, and traveling wave frequency converter) to demonstrate how this general geometric picture can provide insight into specific physical systems.

Keywords: microwave devices, Josephson devices, optical devices

1. Introduction

Reciprocity is the invariance with respect to the exchange of source and detector. Electromagnetic and optical devices (such as isolators and circulators) that break reciprocity are important for their application in several practical contexts [1–4]. Such devices break reciprocal symmetry by exploiting the Faraday effect (i.e., the asymmetry in the propagation velocity of right- and left-circularly polarized light in a magnetic medium subject to an externally applied dc magnetic field). However, because these implementations require large applied magnetic fields that are usually provided by permanent magnets, they are not compatible with an important sub-class of microwave devices: superconducting microwave quantum circuits such as qubits and amplifiers [5]. This raises the more general question of



Content from this work may be used under the terms of the [Creative Commons Attribution 3.0 licence](https://creativecommons.org/licenses/by/3.0/). Any further distribution of this work must maintain attribution to the author(s) and the title of the work, journal citation and DOI.

whether dc magnetic fields are necessary to break reciprocal symmetry at all. Recently, numerous papers have been published showing various realizations of nonreciprocal devices without the need for magnetic materials [5–12]. These examples exploit nonlinear [7, 10, 13, 14] and/or time-variant components and materials [6, 12, 15], using, for example, parametric processes in traveling-wave [6, 9, 15] and lumped-element [5, 11] devices. Although this recent work by other groups has indicated that various coupled-mode systems can implement this same symmetry-breaking without biasing dc magnetic fields, it is not obvious if or how these different systems might be connected conceptually.

In this paper, we discuss the minimal requirements needed to achieve nonreciprocity in a general dual-mode system. This class encompasses most nonreciprocal systems that have been described in the literature, so by studying dual-mode systems, we reach general conclusions about a wide class of nonreciprocal systems. We analyze the conditions under which a general system of two coupled-mode equations behaves nonreciprocally, under only the general assumption of energy and/or photon-number conservation. Our conditions agree with the well-known Lorentz reciprocity theorem in the case of linear, passive, isotropic, time-invariant systems. We achieve this result by employing the well-known Jordan–Schwinger map [16–19] to transform the phase-space of the coupled-mode system into a two-dimensional sphere. As a result, elementary operations on the two modes are described by elements of the symmetry group of the sphere: the special orthogonal group, $SO(3)$, and the group of rotations in three-dimensional space. We show how nonreciprocity arises from the noncommuting properties of these rotations, and we prove some general conditions under which a coupled-mode system is reciprocal. These results are more clearly expressed as geometric conditions on the two-dimensional sphere. Finally, we show how this geometrical description can provide a single theory that allows us to understand the main examples of nonreciprocal devices described in the literature. In particular, in the case of dual-mode nonreciprocal phase shifters, the nonreciprocal phase shift has a geometrical interpretation as the solid angle enclosed by the trajectory of the system on the sphere. While strictly speaking the two-dimensional sphere representation is applicable only when the total photon number is constant, such as in parametric frequency converters, at the end of this paper we discuss a special case involving parametric amplification where a two-dimensional sphere representation can still be applied. We argue that reciprocity in dual-mode systems is a fundamental consequence of the geometric symmetries determined by the coupled-mode phase space.

2. Nonreciprocity in coupled mode systems

In this work, we consider two propagating modes, described by two complex quantities [20], a_1 and a_2 , which satisfy the following set of coupled-mode equations:

$$j\frac{da_1}{dz} = H_{11}a_1 + H_{12}a_2 \quad (1)$$

$$j\frac{da_2}{dz} = H_{21}a_1 + H_{22}a_2, \quad (2)$$

where the system matrix is Hermitian, ($H(z) = H(z)^\dagger$). The right-propagating input modes, $a_1^{R, in}$ and $a_2^{R, in}$, are related to the output modes, $a_1^{R, out}$ and $a_2^{R, out}$, by a matrix, U^R , which

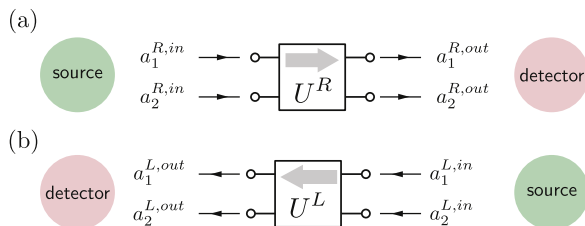


Figure 1. (a) Right- and (b) left-propagating modes and their corresponding four-port representation.

encapsulates the time-evolution of the states under $H(t)$ (see figure 1),

$$a^{R,out} = \begin{bmatrix} a_1^{R,out} \\ a_2^{R,out} \end{bmatrix} = U^R \begin{bmatrix} a_1^{R,in} \\ a_2^{R,in} \end{bmatrix} = U^R a^{R,in}, \quad (3)$$

and similarly for the left-propagating modes U^L ,

$$a^{L,out} = \begin{bmatrix} a_1^{L,out} \\ a_2^{L,out} \end{bmatrix} = U^L \begin{bmatrix} a_1^{L,in} \\ a_2^{L,in} \end{bmatrix} = U^L a^{L,in}. \quad (4)$$

We assume that $U^R, U^L \in SU(2)$, where $SU(2)$ is the group of 2×2 special unitary matrices, and therefore H in equation (1) is in the $\mathfrak{su}(2)$ algebra of 2×2 traceless Hermitian matrices. In the more general case when $U^{R,L} \in U(2)$, we can divide the matrix, $U^{R,L}$, by its determinant. This renormalization corresponds to multiplying $a^{in/out}$ by a global phase factor, and it will not alter the conclusions of this work. This is a four-port transmission problem where the a_1 and a_2 modes may, for instance, represent different propagation paths (illustrated in figure 1), but might also be realized as energy propagating at different wavelengths or frequencies along the same path. More generally, they may be realized as a set of coupled harmonic oscillator modes such as those found in optical, electrical, or mechanical systems, which are not confined to propagating waves [20]. Equation (1) may describe different physical devices, such as mode couplers, ferrite circulators, and parametric frequency converters. The condition $H \in \mathfrak{su}(2)$ implies energy conservation for resonant systems, like mode couplers and ferrite circulators, where $|a_1|^2 + |a_2|^2$ is proportional to the total energy of the system. In the case of nonresonant systems, such as parametric frequency converters, the condition $H \in \mathfrak{su}(2)$ implies photon number conservation instead. What follows depends only on the mathematical properties of equation (1), and not on the specifics of the physical system it describes. We observe here that the conclusions of this work do not apply in general to the case of active devices, such as traveling-wave parametric amplifiers, since in this case $H \in \mathfrak{su}(1, 1)$, and the photon number is not conserved [19]. An exception is provided by the parametric active device in [5], as we will discuss at the end of this paper.

In this work, we are interested in studying the conditions under which the system described by the matrices $\{U^R, U^L\}$ is reciprocal. In general, we define reciprocity as the invariance under the exchange of the input and output modes. However, we can assume that the modes in equations (3) and (4) are determined only up to a constant phase factor. This assumption is true in many physical systems, including the parametric systems mentioned above. Therefore, we say that a coupled-mode system described by the matrices $\{U^R, U^L\}$ is reciprocal if the

following condition is satisfied up to an arbitrary phase shift, ϕ :

$$U^R = Z_\phi U^L Z_\phi^\dagger, \quad (5)$$

where

$$Z_\phi = \begin{bmatrix} e^{-i\phi/2} & 0 \\ 0 & e^{i\phi/2} \end{bmatrix}. \quad (6)$$

The matrix Z_ϕ represents an arbitrary phase shift in the mode basis and makes the definition independent of the particular phase of the input modes. In other words, this definition is gauge-invariant [21, 22]. Furthermore, we observe that reciprocity, as defined in equation (5), is distinct from time-reversal symmetry [4, 21]. Time-reversal symmetry, in fact, would imply that $U^R = (U^L)^T$, which for $U^{R,L} \in SU(2)$ is a special case of (5).

The matrices U^R and U^L can, in general, represent a sequence of individually reciprocal stages, U_k , which may be encoded as a series of elements along a propagation path, each coupling modes ‘1’ and ‘2’ with a corresponding coupling matrix, H_k . In the transmission problem, the direction of propagation establishes the sequence ordering (i.e., $U_R = U_1 U_2 \dots U_n$, while $U_L = U_n U_{n-1} \dots U_1$), where n is the total number of stages. Again, since the coupled modes may also represent a sequence of non propagating (lumped) harmonic oscillator states (i.e., electrical or optical cavity modes), an equivalent sequence ordering may be provided by direct time-domain control of the coupling terms in H . Nonreciprocity originates in asymmetric sequencing of the interactions given by U_k .

If one is concerned only with amplitude reciprocity (i.e., only allowing for nonreciprocal phase shifts in transmission), we have a weaker condition and require only that the absolute value of the left- and right-hand sides of equation (5) are equal; that is, the mode transformations, $U^{L/R}$, are equivalent up to an overall phase.

3. Geometric description of reciprocity

We now derive some general conditions for the reciprocity of a linear coupled two-mode system. In order to do that, we make use of the fact that the states of a coupled-mode system can be geometrically represented as points on a two-dimensional sphere by means of the Jordan-Schwinger map. As discussed in [17], for every state a ($\equiv [a_1 \ a_2]^T$), we can define a real three-component vector, $\vec{r} = a^\dagger \vec{\sigma} a$, where $\vec{\sigma}$ is a symbolic vector with components given by the three Pauli matrices:

$$\sigma_1 = \begin{bmatrix} 0 & 1 \\ 1 & 0 \end{bmatrix}, \quad \sigma_2 = \begin{bmatrix} 0 & -i \\ i & 0 \end{bmatrix}, \quad \sigma_3 = \begin{bmatrix} 1 & 0 \\ 0 & -1 \end{bmatrix}. \quad (7)$$

The vector \vec{r} represents the state of the two-mode system with components $\vec{r} = (2 \operatorname{Re} [a_1^* a_2], 2 \operatorname{Im} [a_1^* a_2], a_1^* a_1 - a_2^* a_2)$. This correspondence is visualized in figure 2. This phase space of the system is constrained to a two-dimensional sphere. The length of the vector \vec{r} is a constant equal to $a^\dagger a$ ($= a_1^* a_1 + a_2^* a_2$), which is the total energy of the modes. If we normalize the total energy to 1, this representation is analogous to the Bloch sphere representation of a two-state quantum system, or to the Poincaré sphere representation of optical polarization states. The cosine of half the elevation angle, ψ , is the fraction of the total power in mode 1, while the azimuthal angle is determined by the relative phase difference between the

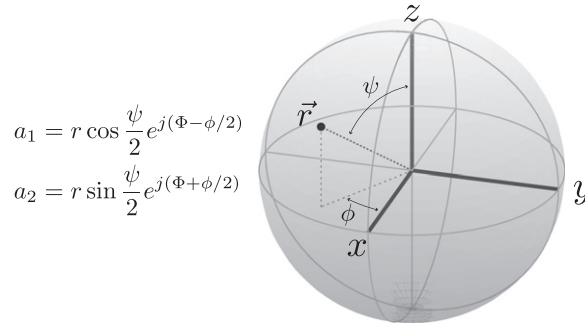


Figure 2. Correspondence between the state of two coupled modes and a point on a two-dimensional sphere. The angle ϕ is equal to the phase difference between the modes, while $\cos(\psi/2)$ is equal to the ratio of the mode amplitudes.

modes. The Jordan–Schwinger map induces the standard map (homomorphism) from the Lie group $SU(2)$ to the special orthogonal group $SO(3)$, which is the group of rotations on a two-dimensional sphere. Under this map, the coupled mode equations (1) assume a compact form,

$$\frac{d\vec{r}}{dz} = \vec{\Omega} \times \vec{r}, \quad (8)$$

where $\vec{\Omega}(z) = (\text{Re}[H_{21}], \text{Im}[H_{21}], (H_{11} - H_{22})/2)$. In this representation, the mode transformations, $U^{R/L}$ in equations (3) and (4), can now be described by rotations around the corresponding vectors, $\vec{\Omega}_{R/L}$, in three-dimensional space. In particular, any $SU(2)$ transformation can be expressed as

$$U(\theta, \hat{n}) = I_2 \cos(\theta/2) - i \sin(\theta/2) \hat{n} \cdot \vec{\sigma} = e^{-i\frac{\theta}{2} \hat{n} \cdot \vec{\sigma}}. \quad (9)$$

The $SU(2)$ transformation (9) of the state a corresponds to the $SO(3)$ three-dimensional rotation of \vec{r} by an angle, θ , around the vector \hat{n} . In the following, we refer to $U(\theta, \hat{n})$ as representing a rotation around \hat{n} , without explicitly mentioning the corresponding 3×3 $SO(3)$ matrix. Here, \hat{n} is a unit vector parallel to $\vec{\Omega}$, and θ is the total phase accumulated as the system evolves under $H(z)$. It is worthwhile to note that, if we replace the position variable, z , with a time variable, t , equation (8) can also be interpreted as the equation of motion for spin angular momentum (\vec{r}) in an applied magnetic field ($\vec{\Omega}$), connecting the dual-mode transformations to the Bloch sphere dynamics familiar from nuclear magnetic resonance and quantum computing. It is therefore no surprise that equation (9) yields the familiar Bloch rotations from these fields. We emphasize, however, that this representation is also valid (and useful) for classical oscillators.

For our purposes, the benefit of this geometric mapping is that it recasts the reciprocity condition (equation (5)) as a condition on the $SO(3)$ rotation matrices corresponding to the transformations, $U^{R/L}$. Furthermore, any condition on these transformations can likewise be applied to the associated effective rotation generator vectors, $\hat{n}^{R/L}$. To begin with, we recognize Z_ϕ in equation (5) as a rotation around the z -axis by $\phi/2$, $U(\phi, \hat{z})$. Therefore, by equation (5), the mode transformations, $U^{R/L}$, are reciprocal if and only if their associated rotation generators, $\hat{n}^{R/L}$, can be transformed into one another by a simple z -rotation (see figure 3). Additionally, the weaker condition for maintaining amplitude reciprocity alone (i.e., that the absolute values of

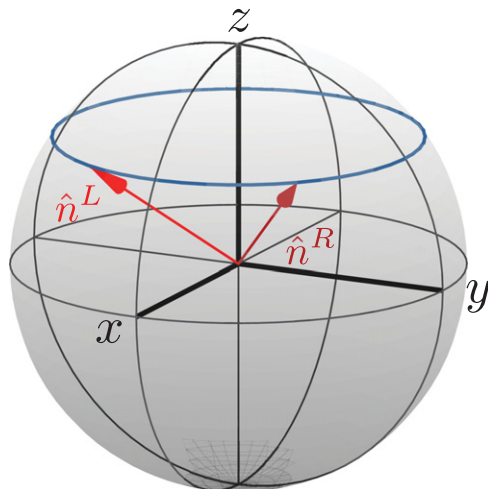


Figure 3. A device described by two rotations around the vectors $\vec{\hat{n}}^R$ and $\vec{\hat{n}}^L$ is reciprocal if and only if the rotation angles are the same and $\vec{\hat{n}}^R$ and $\vec{\hat{n}}^L$ can be transported onto each other by a rotation around the z -axis.

both sides of equation (5) are equal), is satisfied if \hat{n}^R and \hat{n}^L can be related by a z -rotation followed by reflection across the xy -plane.

3.1. Reciprocity

In this same spirit, we are now able to state some general conditions for reciprocity in coupled-mode systems that undergo a sequence of mode transformations. We assume that the mode transformation matrix is given by the product of rotations around the ordered sequence of vectors, $\vec{\Omega}_1 \dots \vec{\Omega}_n$, in the forward direction, corresponding to a single effective rotation vector, $\vec{\Omega}^R$, and around the reverse sequence, $\vec{\Omega}_n \dots \vec{\Omega}_1$, in the backward direction, corresponding to an effective rotation vector, $\vec{\Omega}^L$. We show in appendix A that if the rotation vectors, $\vec{\Omega}_1 \dots \vec{\Omega}_n$, lie on a plane, P , the associated effective rotation generator unit vectors, \hat{n}^R and \hat{n}^L , are symmetrical with respect to the same plane, P . We can therefore conclude that if $\vec{\Omega}_1, \dots, \vec{\Omega}_n$ lie on a plane containing the z -axis, any forward or reverse sequence composed of this set of rotation vectors is always reciprocal. The converse is, in general, not true; however, as discussed in appendix A, a reciprocal system can always be implemented by means of a set of rotation vectors lying in the xz -plane. Therefore, devices which implement only rotations with axes lying on the xz -plane represent the most general class of coupled-mode reciprocal systems. This condition can be translated back into the original $SU(2)$ picture, and it corresponds to the fact that the coupled-mode system matrix, H , in equation (1) can be expressed as a linear combinations of the σ_1 and σ_3 Pauli matrices, apart from an irrelevant Z_ϕ transformation. By this reasoning, reciprocity is always maintained if the rotation vectors are all collinear, since this is a special case of this coplanar/ z -axis constraint.

3.2. Gyration

If a generic set of rotation vectors, $\vec{\Omega}_1, \dots, \vec{\Omega}_n$, lie in the xy -plane, then the vectors \hat{n}^R and \hat{n}^L are symmetric with respect to the xy -plane and the system behaves as a nonreciprocal phase shifter

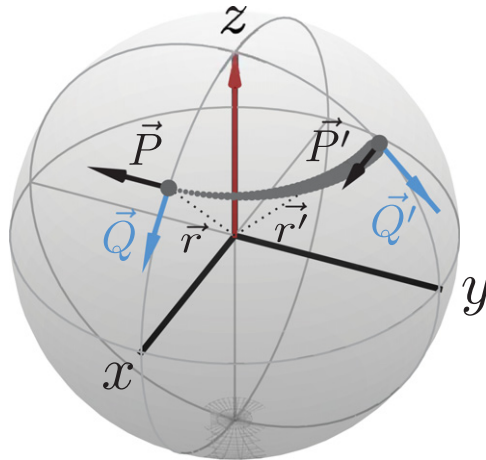


Figure 4. The angle of rotation of the tangent vector to the sphere is equal to twice the common phase shift accumulated by the modes. The sign of the phase is positive if the vector, \vec{P} , rotates counter-clockwise around the position vector, \vec{r} .

or a gyrator. The system is reciprocal only in the special case when $\hat{n}^R = \hat{n}^L$. Finally, amplitude nonreciprocity can be obtained only if the set of rotation vectors do not all lie in the same horizontal or vertical plane.

3.3. Geometric phase

In figure 2, we see that the geometric representation of the position of the sphere depends on the relative amplitude and differential phase shift between the modes. However, a gyrator is characterized by a difference in the total phase shift of the modes. In the next section, we will study an example of a device implementing a physical gyrator, and for this we need to know how the common phase is encoded in the geometric representation. The answer is shown in figure 4; this discussion closely follows Berry's own discussion in [23]. If we consider two orthogonal unit tangent vectors \vec{P} and \vec{Q} to the sphere at \vec{r} such that $\vec{P} \times \vec{Q} = \vec{r}$, and if we assume that the vectors \vec{P} , \vec{Q} , and \vec{r} evolve according to equation (8), then a common phase shift, ϕ , of the modes causes a rotation of the vectors \vec{P} and \vec{Q} by 2ϕ in the tangent plane at \vec{r} . Therefore, while \vec{r} doesn't depend on the common phase shift, \vec{P} and \vec{Q} do. The direction of the rotation is set by \vec{r} ; a π phase shift corresponds to a counter-clockwise 2π rotation of \vec{P} around \vec{r} . More generally, the rotation angle is made up of two components: the radial component of the instantaneous rotation axis that generates twists around the current position vector \vec{r} and the tangent component that generates the parallel transport of \vec{P} along the path on the sphere. The phase shift resulting from the second component, known as the 'geometric phase', is dependent only on the particular path covered on the sphere. The latter constitutes the nonreciprocal phase contribution in nonreciprocal phase shifters, as described in more detail below. The ability to interpret phase nonreciprocity in terms of a geometrical gauge-invariant quantity is, we think, an advantage of the geometric representation provided in this work over other representations, such as the one used in [5], where the evolution of a two-mode device is visually described by the rotation and squeezing of the modulation ellipse in the quadratures plane.

3.4. Parametric coupling and $\vec{\Omega}$

So far, we have not addressed the specific nature of the coupling between modes ‘1’ and ‘2’. In particular, if the coupling terms $H_{12/21}$ are static, they cannot hold phase information. In this case, the modes cannot be coupled unless they are resonant, and the effective rotation vector $\vec{\Omega}$ lies completely along the \hat{x} direction. However, if the modes are nonresonant, they can exchange energy if $H_{12/21}$ are modulated at the difference frequency. This corresponds to the well-known concept of parametric frequency conversion, and it has the advantage of holding an arbitrary phase that is determined by an external ‘pump’ drive that modulates the coupling terms. With parametric frequency conversion, $\vec{\Omega}$ is then directed anywhere in the equatorial plane of the Poincaré sphere, while any detuning from the difference frequency condition will tip $\vec{\Omega}$ out of this plane. From the geometric constraints outlined above, it follows that parametric frequency conversion generates the possibility of breaking reciprocity by creating sequences of unitary stages with effective rotation generators, \hat{n}_k , that are not constrained to the xz -plane.

4. Applications

In this section, we apply the theory described above to the analysis of different examples of reciprocal and nonreciprocal devices. The geometric picture offers a tool to understand the common operating principle of very different physical implementations of nonreciprocity.

4.1. Real system matrix, directional couplers

The first case we consider is a real coupled-mode system matrix H ,

$$H = \begin{bmatrix} \omega_1 & g(z) \\ g(z) & \omega_2 \end{bmatrix}, \quad (10)$$

where g , ω_1 , and ω_2 are real. Such a system, for example, describes directional couplers and beam splitters (where the coupling coefficient is static) or a sequence of parametric converters with a non-propagating stationary pump (where the coupling coefficient is time-dependent, but the phase is constant in space). The rotation vector in equation (8) corresponding to this system is $\vec{\Omega}(z) = (g(z), 0, (\omega_2 - \omega_1)/2)$, and it is located in the xz -plane. Therefore, these systems are always reciprocal, and we proved the following result: Any dual-mode system with a stationary coupling coefficient is reciprocal. It is important to observe that this conclusion remains valid for nonlinear coupled-mode systems when the coupling coefficient, $g(z, \vec{a})$, is a function of the mode amplitudes. When equation (10) describes a two-mode electromagnetic system, the special static case where g is constant corresponds to a linear, isotropic, time-invariant system, which satisfies the hypothesis of Lorentz reciprocity [1, 24]. The system (10) is an example of a more general class of time-variant reciprocal systems.

4.2. Nonreciprocal phase shifters

A nonreciprocal phase shifter can be implemented with a sequence of two ideal microwave mixers, as discussed in [25]. The mixers act as frequency converters between two modes at frequency ω and $\omega + \omega_p$, where ω_p is the frequency of the local oscillator feeding the mixer. The first mixer up-converts a signal mode at frequency ω to the frequency $\omega + \omega_p$, while the second mixer down-converts the signal back to the frequency ω . The phases of the local

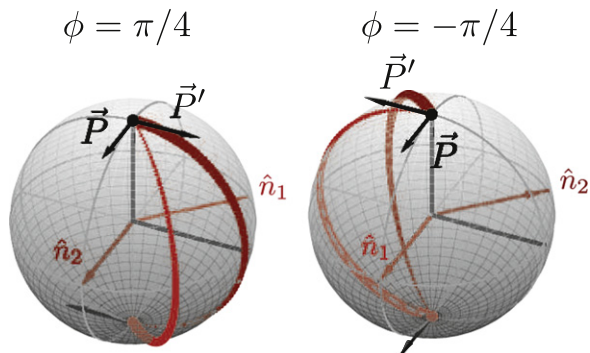


Figure 5. A gyrator can be obtained by a sequence of 2π rotations around the axes shown in the figure. Depending on the order of the rotations, a $\pm\pi/4$ phase shift is obtained and the tangent vector, \vec{P} , is rotated by $\pm\pi/2$. In this particular case, where the axis of rotation is always orthogonal to the position vector \vec{r} , the total phase shift is equal to the geometric phase due to the parallel transport of \vec{P} on the surface of the sphere.

oscillator at the two mixers are ϕ_1 and ϕ_2 , respectively, with $\phi_1 \neq \phi_2$. The action of each mixer on the two modes at frequencies ω and $\omega + \omega_p$ can be represented by means of the following matrix:

$$U(\pi, \cos \phi_i \hat{x} + \sin \phi_i \hat{y}) = \begin{bmatrix} 0 & e^{-j\phi_i} \\ e^{j\phi_i} & 0 \end{bmatrix}. \quad (11)$$

Each mixer therefore acts by a rotation on the sphere by an angle, π , around the axis, $(\cos(\phi_i), \sin(\phi_i), 0)$. By cascading two mixers, we obtain a gyrator that operates as shown in figure 5, with nonreciprocal phase shifts, $\pm(\phi_2 - \phi_1)$, depending on the direction of propagation. We also observe in figure 5 that the tangent vector, \vec{P} , covers a closed loop and is rotated by an angle equal to $2(\phi_2 - \phi_1) = \pi/2$ in the forward propagation and $-\pi/2$ in the backward propagation. Since the rotation axis is constantly orthogonal to the position vector, \vec{r} , the nonreciprocal phase shift is due entirely to the geometric contribution that we discussed before. In particular, we conclude that the solid angle enclosed by the path on the sphere covered by the system is equal to the nonreciprocal phase shift accumulated in the device. Physical intuition for why the geometric phase gives a nonreciprocal contribution in parametric systems can be obtained by comparing this problem with the propagation of light in a lossless chiral medium, such as a twisted fiber. In both cases, the rotation of the polarization state can be described by the parallel transport of a point on the unit sphere. However, in the chiral medium, the path covered on the unit sphere does not depend on the direction of propagation, and the accumulated geometric phase is independent of the direction of propagation. In parametric systems, the sign of the geometric phase depends on the direction of evolution of the pump phase with respect to the signal.

4.3. Parametric frequency converters

Another type of nonreciprocal device is obtained by exploiting parametric interactions. For example, nonreciprocity can be obtained in traveling-wave devices [6] where two modes at different frequencies interact through a traveling-wave perturbation (a pump signal), as shown

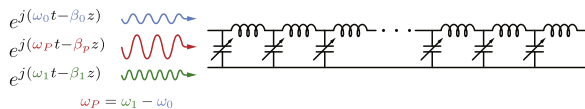


Figure 6. Nonreciprocal traveling-wave parametric frequency converter. A pump at frequency ω_c generates parametric coupling between two modes at frequencies $\omega_{1,2}$, such that $\omega_2 - \omega_1 = \omega_p$. Frequency conversion is obtained under phase-matching conditions in the case of a copropagating pump, but not in the counter-propagating case.

in figure 6. The direction of the traveling pump wave generates a nonreciprocal behaviour by creating a preferential direction of propagation. This type of device can be described by the following coupled-mode system:

$$j \frac{da_1}{dz} = \beta_1 a_1 + g e^{j(\beta_p z + \phi_p)} a_2, \quad (12)$$

$$j \frac{da_2}{dz} = g e^{-j(\beta_p z + \phi_p)} a_1 + \beta_2 a_2, \quad (13)$$

where the coupling coefficient, g , is proportional to the amplitude of the traveling-wave perturbation, and ϕ_p is the phase of the perturbation. The time-dependent perturbation can be obtained, for example, by using diodes [6], nonlinear materials [7, 13], or Josephson junctions [5]. The system (12) can be described by our geometrical model. The state of the system evolves on the sphere by rotating around the instantaneous axis, $\vec{\Omega}(z) = \{2g \cos(\beta_p z + \phi_p), 2g \sin(\beta_p z + \phi_p), \beta_2 - \beta_1\}$. This vector spans a vertical cone, and nonreciprocity is obtained if $\beta_1 \neq \beta_2$ because the vector is not fully contained in any vertical or horizontal plane. We can verify amplitude nonreciprocity directly by calculating the effective rotation vectors, $\vec{\Omega}^\pm$, which describe propagation over a finite length of line in the right (–) and left (+) directions. By moving into a reference frame rotating at the pump frequency, we see that $\vec{\Omega}^\pm = \{2g, 0, \beta_2 - \beta_1 \pm \beta_p\}$. Under the phase matching condition, $\beta_p = \beta_2 - \beta_1$, for the forward propagating (–) case, full mode conversion is obtained after a distance, $z = \pi/2g$. In the reverse direction, no mode conversion is obtained if $\beta_p \gg g$, because $\vec{\Omega}^+$ is approximately parallel to the z -axis in this case. Therefore, the device acts as an isolator.

Another type of nonreciprocal device based on Josephson parametric converters is described in [5]. This device, shown in figure 7(a), is made of two up-down converter stages that employ the nonlinearity of Josephson junctions to mix two signals, a_1 and a_2 , at frequency ω_0 with a pump at frequency ω_p , and to generate two output signals, b_+ and b_- , at frequencies $\omega_\pm = \omega_0 \pm \omega_p$. Parametric converters are non-Hermitian devices and therefore cannot be described, in general, by $SU(2)$ transformations alone. The same geometric reasoning can be extended to non-Hermitian devices. In the case of parametric amplifiers, for example, the state of the system can be represented by a point on a hyperbolic surface instead of a sphere. We will not analyze this extension here, and we observe that in the particular case of the device in figure 7(a), the Bloch sphere representation turns out to be suitable, as we discuss below. The Josephson parametric converters are four-port devices, but we can renormalize the scattering matrix with respect to an appropriate set of port impedances and add suitable reciprocal impedance matching networks in order to cancel the reflected waves at every port [26, 27]. As a result, the transmission coefficients across the up-down converters can be described by cascading the two 2×2 renormalized off-diagonal blocks, U_L and U_R . In particular, after

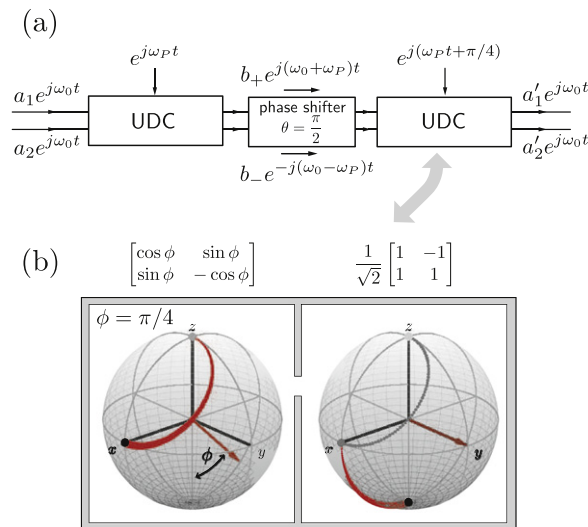


Figure 7. (a) Scheme of the four-port circulator from [5]. Circulation is achieved through parametric conversion into an auxiliary mode basis, b_+ , b_- , at frequencies $\omega_{\pm} = \omega_0 \pm \omega_p$. (b) Bloch sphere representation of the elementary up/down converter stage. The phase shift, ϕ , is equal to the phase of the pump signal in (a). The particular state trajectory shown corresponds to an initial state entirely in the a_1 mode propagating to the right.

performing a $\pi/2$ rotation of the b_{\pm} basis, we can rewrite the up-down converter transfer matrices as

$$U'_L = (1 - i)\sqrt{\tilde{s}_d\tilde{t}_d}U(\pi/2, \hat{y})U(\pi/2, \hat{n}_\phi)L_y, \quad (14)$$

$$U'_R = (1 - i)\sqrt{\tilde{s}_u\tilde{t}_u}L_yU(\pi/2, \hat{n}_\phi)U(\pi/2, \hat{y}), \quad (15)$$

where $\tilde{s}_{d,u}$ and $\tilde{t}_{d,u}$ are constant coefficients defined in appendix B, and L_y is a y -axis ‘Lorentz boost’,

$$L_y = U(\pi/2, \hat{x})L_zU(\pi/2, -\hat{x}) = U(\pi/2, \hat{x}) \begin{bmatrix} \sqrt{k_{st}} & 0 \\ 0 & \sqrt{\frac{1}{k_{st}}} \end{bmatrix} U(\pi/2, -\hat{x}). \quad (16)$$

The operation of the up-down converter in figure 7(a) can be described by the sequence of rotations in figure 7(b). In this equivalent description, the up (down) converter stage performs a $\pi/2$ rotation around the y -axis followed (preceded) by a rotation around a vector lying on the xz -plane at an angle, ϕ , with the negative z -axis. The amplification is factored out as a separate Lorentz boost, L_y . Somewhat surprisingly, the Lorentz boost, which is equivalent to a rescaling of the Bloch sphere, does not have any impact on the nonreciprocal operation of the four-port circulator in figure 8. In fact, it is clear from figure 8 that the boost operation is performed when the system is either on the y -axis or on the great circle orthogonal to the y -axis. In both these cases, the boost, L_y , causes a rescaling of the mode amplitudes without any effect on the relative phase between the modes or their relative power distribution. In other words, if the modes have equal initial photon numbers at the moment the amplification operation is performed, the photon

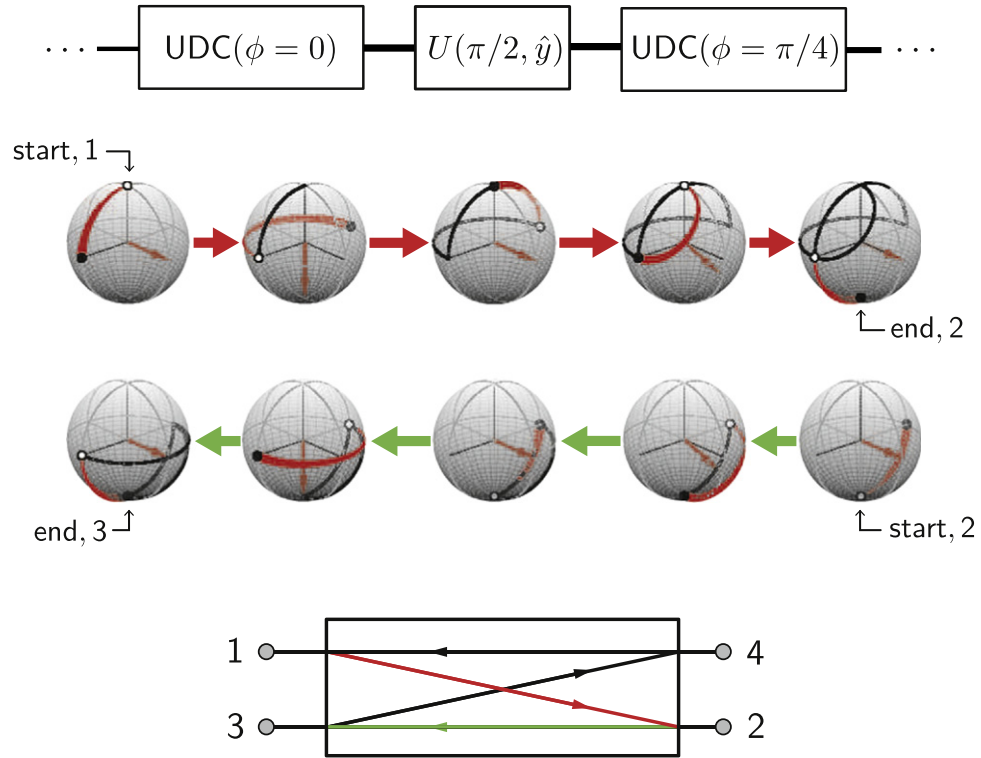


Figure 8. Description of the device shown in figure 7(a) as a sequence of elementary rotation operations. The empty circle represents the input state and the closed circle represents the output state after each elementary transformation. Propagation from left to right (shown on the top) causes full mode conversion from mode 1 to 2, while propagation of mode 2, from right to left, causes no mode conversion as a result of the inversion in the order of the elementary rotations.

numbers will be the same after amplification as well. This very particular property of the device in figure 7 allows us to employ a simplified Bloch sphere description of the device’s nonreciprocal behaviour.

4.4. Magnetized ferrites

Ferrite devices are a well-known example of nonreciprocal devices. Nonreciprocity is a consequence of an anisotropic magnetic susceptibility tensor, μ , in the presence of a high magnetic bias field. For a transverse electromagnetic wave (TEW) traveling through the ferrite medium, the magnetic field is given by $\vec{H}(z, t) = \vec{h}e^{j(\beta z - \omega t)}$ and the electric field is $\vec{E} = \sqrt{\mu_0/\epsilon_0} \vec{k} \times \vec{H}$, and from Maxwell’s equations,

$$-\frac{\partial \vec{M}}{\partial t} - \mu_0 \frac{\partial \vec{H}}{\partial t} = \nabla \times \vec{E} = j\beta \sqrt{\frac{\mu_0}{\epsilon_0}} \vec{k} \times \vec{H}. \quad (17)$$

In a ferrite medium, the magnetization vector \vec{M} satisfies the equation $\partial \vec{M} / \partial t = \gamma \vec{M} \times \vec{H}$, where γ is the gyromagnetic ratio [1]. After simplifying and removing the $\beta z - \omega t$ dependence, we obtain

$$\frac{\partial \vec{h}}{\partial t} = \gamma \vec{M} \times \vec{h}. \quad (18)$$

The magnetic vector field rotates around the magnetization vector \vec{M} and equation (18) is formally identical to equation (8). Therefore, the Bloch sphere picture provides a useful insight into the similarity between nonreciprocal coupled-mode systems and anisotropic devices. Here, the magnetization vector \vec{M} has the same role as the pump signal in parametric devices. More generally, it can be shown that the evolution of the polarization of an electromagnetic wave in a linear or nonlinear birefringent medium can also be described by equation (8) [28]. As for the traveling-wave parametric frequency converter discussed in the previous section, nonreciprocity in a ferrite medium arises from the fact that the direction of the vector \vec{M} is reversed upon inversion of the direction of propagation of the electromagnetic signal, and as a result, the global rotation angle of the magnetic field vector \vec{H} is also reversed.

5. Conclusions

In this work, we introduced a general geometric description of reciprocity in coupled-mode systems. This model is applicable to any dual-mode system, no matter the physical nature of the modes, provided that its energy and/or photon number is conserved. As a result, we were able to describe the mode transformation by different nonreciprocal systems as a sequence of noncommuting rotations in three-dimensional space. In this picture, the state of the system is represented by a point on a two-dimensional sphere, similar to the Bloch sphere employed to describe the evolution of the polarization vector of light or of an elementary quantum bit. We further proved general statements on the minimal requirements to achieve nonreciprocity in coupled-mode systems. In particular, we concluded that at least two elementary rotation stages are required for nonreciprocity, and the rotation axes cannot all lie on a vertical plane (i.e., a plane joining the north and south pole of the sphere). This simple condition explains the nonreciprocal behaviour of a very large class of devices, including ferrite-based waveguides, parametric devices, and Kerr media.

Appendix A. Proof of general reciprocity conditions

Assume that $\vec{r}_{1\dots N}$ are N vectors in \mathfrak{R}^3 . Let us consider the rotations $R_i \in SO(3)$ around the vector \vec{r}_i by an angle, θ_i . We write $R_N^R = R_1 R_2 \dots R_N$ and $R_N^L = R_N R_{N-1} \dots R_1$. Let us denote the axes of rotations corresponding to $R_N^{L,R}$ with $\vec{n}_N^{L,R}$. In general, $\vec{n}_N^L \neq \vec{n}_N^R$, unless the N rotation axes are coincident. We can prove the following theorem: If $\vec{r}_{1\dots N}$ lie in the same plane P , then R^L and R^R are rotations of the same angle, and the axes of rotation, \vec{n}_N^R and \vec{n}_N^L , are symmetrical with respect to the plane P .

We can prove this result by induction on the number of vectors. The theorem is obviously valid for $N = 1$. Let us assume now that the theorem is valid for the $N - 1$ vectors, $\vec{r}_{1\dots N-1}$. Then the rotation axes, \vec{n}_{N-1}^L and \vec{n}_{N-1}^R , are symmetrical with respect to P and can be expressed as

$$\vec{n}_{N-1}^L = \vec{n}_{\parallel} + \vec{n}_{\perp}, \quad \vec{n}_{N-1}^R = \vec{n}_{\parallel} - \vec{n}_{\perp}, \quad (A.1)$$

for two suitable vectors, $n_{\perp} \perp P$ and $n_{\parallel} \parallel P$. From [29], if two rotations around the axes \vec{u} and \vec{v} are multiplied in order, the composite rotation has axis $\vec{w} = \alpha(\theta_u)\vec{u} + \beta(\theta_v)\vec{v} + \gamma(\theta_u, \theta_v)\vec{u} \times \vec{v}$. Moreover, $\gamma(\theta_u, \theta_v) = \gamma(\theta_v, \theta_u)$. Therefore, we can calculate the composite of the N rotations

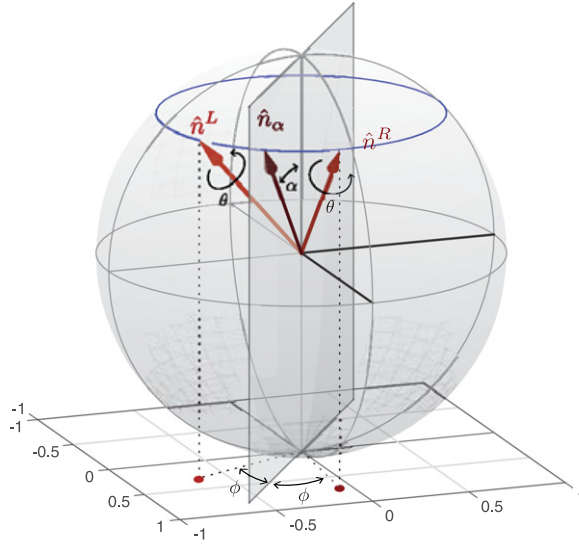


Figure A1. A reciprocal device described by the rotations with angle θ around the vectors \hat{n}^L and \hat{n}^R for left-to-right and right-to-left propagation, respectively, is equivalent to the sequence of rotations, $U(\theta, \hat{n}^L) = Z_\phi^{-1} U(\theta, \hat{n}^\alpha) Z_\phi$ (for the left-to-right propagation), where Z_ϕ is a counter-clockwise rotation by an angle ϕ around the z -axis, and $U(\theta, \hat{n}^R)$ is a rotation by an angle θ around the vector \hat{n}^R in the figure.

$\vec{r}_{1\dots N}$ as

$$\vec{n}_N^L = \alpha \vec{n}_{N-1}^L + \beta \vec{r}_n + \gamma \vec{n}_{N-1}^L \times \vec{r}_n \quad (\text{A.2})$$

$$\begin{aligned} &= (\alpha \vec{n}_\parallel + \beta \vec{r}_n + \gamma \vec{n}_\perp \times \vec{r}_n) \\ &\quad + (\alpha \vec{n}_\perp + \gamma \vec{n}_\parallel \times \vec{r}_n) \end{aligned} \quad (\text{A.3})$$

$$\vec{n}_N^R = \alpha \vec{n}_{N-1}^R + \beta \vec{r}_n + \gamma \vec{r}_n \times \vec{n}_{N-1}^R \quad (\text{A.4})$$

$$\begin{aligned} &= (\alpha \vec{n}_\parallel + \beta \vec{r}_n + \gamma \vec{n}_\perp \times \vec{r}_n) \\ &\quad - (\alpha \vec{n}_\perp + \gamma \vec{n}_\parallel \times \vec{r}_n), \end{aligned} \quad (\text{A.5})$$

where in the second step we separated the vectors into their components parallel and orthogonal to P . It follows from equation (A.2) that \vec{n}_N^L and \vec{n}_N^R are also in the form (A.1) and are therefore symmetrical with respect to the plane P .

We can further prove that if a system is described by a couple of vectors, \vec{n}^L and \vec{n}^R for the forward and backward propagation that are symmetric with respect to a plane P , then the system can always be described by means of a sequence of elementary rotations lying on P . In fact, let us assume that \vec{n}^L and \vec{n}^R are placed as shown in figure A1. Then the system can be described in the forward direction by means of the sequence of rotations, $U(\theta, \hat{n}^L) = Z_\phi^{-1} U(\theta, \hat{n}^\alpha) Z_\phi$, and by the inverse sequence from right to left. Z_ϕ is a rotation by an angle, ϕ , around the z -axis. Therefore, any reciprocal device can be built by employing three rotations around axes lying in the xz -plane, up to an irrelevant phase change.

Appendix B. Description of the parametric lumped element isolator by a sequence of three-dimensional rotations

In order to derive the group of transformations that describes the device in figure 7(a), we can start from the 4×4 scattering matrix representation of the device, which relates the incoming wave amplitudes, $[a_1^{in}, a_2^{in}, b_+^{in}, b_-^{in}]$, to the corresponding outgoing ones [5]:

$$S_{UDC} = \begin{bmatrix} r_0 & -q_0 & t_d e^{-i\phi} & s_d e^{i\phi} \\ q_0 & r_0 & i t_d e^{-i\phi} & -i s_d e^{i\phi} \\ t_u e^{i\phi} & -i t_u e^{i\phi} & r_+ & 0 \\ -s_u e^{-i\phi} & -i s_u e^{-i\phi} & 0 & r_- \end{bmatrix}, \quad (\text{B.1})$$

where ϕ is the pump phase, and explicit expressions for the remaining other parameters are provided in [5]. We can proceed by renormalizing the scattering matrix with respect to a suitable set of port impedances. As a result, the reflection coefficients become zero in the new impedance environment, and the scattering matrix can be expressed as

$$\tilde{S}_{UDC} = \begin{bmatrix} Q & U_L \\ U_R & 0 \end{bmatrix}, \quad (\text{B.2})$$

where

$$Q = \begin{bmatrix} 0 & -q_0 \\ q_0 & 0 \end{bmatrix}. \quad (\text{B.3})$$

The two off-diagonal blocks can be written as a product of a scalar factor and a 2×2 complex matrix with unit determinant,

$$U_L = (1 - i) \sqrt{\tilde{s}_d \tilde{t}_d} \begin{bmatrix} k_{st} \frac{i+1}{2} e^{-i\phi} & \frac{1}{k_{st}} \frac{i+1}{2} e^{i\phi} \\ k_{st} \frac{i-1}{2} e^{-i\phi} & \frac{1}{k_{st}} \frac{1-i}{2} e^{i\phi} \end{bmatrix}, \quad (\text{B.4})$$

$$U_R = (1 - i) \sqrt{\tilde{s}_u \tilde{t}_u} \begin{bmatrix} k_{st} \frac{i+1}{2} e^{i\phi} & k_{st} \frac{1-i}{2} e^{i\phi} \\ -\frac{1}{k_{st}} \frac{i+1}{2} e^{-i\phi} & \frac{1}{k_{st}} \frac{1-i}{2} e^{-i\phi} \end{bmatrix}, \quad (\text{B.5})$$

where $k_{st} = \sqrt{\tilde{t}_u \tilde{s}_u} = \sqrt{\tilde{t}_d \tilde{s}_d} \cdot \tilde{s}_{u,d}$ and $\tilde{t}_{u,d}$ are renormalized transmission coefficients, and they do not depend on the pump phase, ϕ . The matrix, Q , describes the direct coupling between modes a_1 and a_2 , while the 2×2 matrices (B.4) describe transmission through the up-down converter in the left and right directions; they are not unitary. From the form of equation (B.2), it is clear that we can compute the transmission coefficients in the device in figure 8 by multiplication of the 2×2 off-diagonal blocks (B.4). We now consider the group of 2×2 complex matrices with unit determinants, called the special linear group, $SL(2, \mathbb{C})$. During our previous discussion, we observed that the symmetry group of a two-mode system with a single

parametric frequency conversion process is $SU(2)$, and this group can be mapped onto the three-dimensional rotation group, $SO(3)$, via the Jordan–Schwinger map. In analogy to our previous discussion, we observe that $SL(2, \mathbb{C})$ can be mapped onto the Lorentz group, $SO(3, 1)$, via the spinor representation map [30]. The spinor map associates to every four-vector $\hat{r} = (r_0, r_1, r_2, r_3)$ a Hermitian matrix, X_r , given as

$$X_r = \begin{bmatrix} r_0 + r_3 & r_1 - ir_2 \\ r_1 + ir_2 & r_0 - r_3 \end{bmatrix}. \quad (\text{B.6})$$

We further assume that the matrix (B.6) has a unit determinant (i.e. $r_0^2 - r_1^2 - r_2^2 - r_3^2 = 1$). As a result, we can map the matrix, $U \in SL(2, \mathbb{C})$, onto the Lorentz transformation, $L_U \in SO(3, 1)$, such that $\hat{r}' = L_U \hat{r}$ iff $X_{r'} = UX_r U^\dagger$. Since the Lorentz group is the symmetry group of hyperbolic space, we could give a geometric representation of the state of the device in figure 7(a) as a point in such hyperbolic space, defined by the position four-vector, \hat{r} . However, a simpler description on the Bloch sphere is also possible, because the matrices, $U_{L,R}$, can be decomposed in the following way:

$$U_L = (1 - i)\sqrt{s_d t_d} U(\pi/2, \hat{y}) U(\pi/2, \hat{n}_\phi) U(\pi/2, \hat{x}) L_z, \quad (\text{B.7})$$

$$U_R = (1 - i)\sqrt{s_u t_u} L_z U(-\pi/2, \hat{x}) U(\pi/2, \hat{n}_\phi) U(\pi/2, \hat{y}), \quad (\text{B.8})$$

where

$$L_z = \begin{bmatrix} \sqrt{k_{st}} & 0 \\ 0 & \sqrt{\frac{1}{k_{st}}} \end{bmatrix}. \quad (\text{B.9})$$

The decomposition (B.7) consists only of unitary transformations, which correspond to three-dimensional rotations of the Bloch sphere, and the $SL(2, \mathbb{C})$ representation of a z -axis Lorentz boost, L_z , which corresponds to a rescaling of the Bloch sphere. Finally, by performing a $\pi/2$ rotation of the b_\pm basis, we can rewrite the up-down converter transfer matrices in equation (B.7) as in equation (14), and represented in figure 7(b).

References

- [1] Pozar D M 2005 *Microwave Engineering* 3rd edn (Hoboken, NJ: Wiley) pp 497–511
- [2] Fay C and Comstock R 1965 Operation of the ferrite junction circulator *IEEE Trans. Microw. Theory Tech.* **13** 15–27
- [3] Fan S *et al* 2012 Comment on nonreciprocal light propagation in a silicon photonic circuit *Science* **335** 38–38
- [4] Potton R 2004 Reciprocity in optics *Rep. Prog. Phys.* **67** 717
- [5] Kamal A, Clarke J and Devoret M 2011 Noiseless non-reciprocity in a parametric active device *Nat. Phys.* **7** 311–5
- [6] Lira H, Yu Z, Fan S and Lipson M 2012 Electrically driven nonreciprocity induced by interband photonic transition on a silicon chip *Phys. Rev. Lett.* **109** 033901
- [7] Kaplan A 1983 Light-induced nonreciprocity, field invariants, and nonlinear eigenpolarizations *Opt. Lett.* **8** 560–2
- [8] Shvets G 2012 Not every exit is an entrance *Physics* **5** 78

- [9] Abdo B, Sliwa K, Frunzio L and Devoret M 2013 Directional amplification with a Josephson circuit *Phys. Rev. X* **3** 031001
- [10] Gallo K, Assanto G, Parameswaran K R and Fejer M M 2001 All-optical diode in a periodically poled lithium niobate waveguide *Appl. Phys. Lett.* **79** 314–6
- [11] Kamal A 1960 A parametric device as a nonreciprocal element *Proc. IRE* **48** 1424–30
- [12] Longhi S 2013 Effective magnetic fields for photons in waveguide and coupled resonator lattices *Opt. Lett.* **38** 3570–3
- [13] Fan L *et al* 2013 Silicon optical diode with 40 db nonreciprocal transmission *Opt. Lett.* **38** 1259–61
- [14] Chang L *et al* 2014 Parity-time symmetry and variable optical isolation in active-passive-coupled microresonators *Nat. Photonics* **8** 524–9
- [15] Fang K, Yu Z and Fan S 2012 Realizing effective magnetic field for photons by controlling the phase of dynamic modulation *Nat. Photonics* **6** 782–7
- [16] Feynman R P, Vernon F L Jr and Hellwarth R W 2004 Geometrical representation of the schrödinger equation for solving maser problems *J. Appl. Phys.* **28** 49–52
- [17] Frigo N 1986 A generalized geometrical representation of coupled mode theory *IEEE J. Quantum Electron.* **22** 2131–40
- [18] Leonhardt U 2010 *Essential Quantum Optics: from Quantum Measurements to Black Holes* (Cambridge: Cambridge University Press)
- [19] Yurke B, McCall S L and Klauder J R 1986 Su (2) and su (1, 1) interferometers *Phys. Rev. A* **33** 4033
- [20] Louisell W H 1960 *Coupled Mode and Parametric Electronics* (New York: Wiley)
- [21] Deák L and Fülöp T 2012 Reciprocity in quantum, electromagnetic and other wave scattering *Ann. Phys., NY* **327** 1050–77
- [22] Leung P T and Young K 2010 Gauge invariance and reciprocity in quantum mechanics *Phys. Rev. A* **81** 032107
- [23] Berry M 1990 *Quantum Adiabatic Anholonomy* (Naples: Bibliopolis) pp 125–81
- [24] Lorentz H 1896 The theorem of poynting concerning the energy in the electromagnetic field and two general propositions concerning the propagation of light *Amsterdammer Akademie der Wetenschappen* **4** 176
- [25] Fang K, Yu Z and Fan S 2013 Experimental demonstration of a photonic Aharonov-Bohm effect at radio frequencies *Phys. Rev. B* **87** 60301
- [26] Wallace J W and Jensen M A 2004 Mutual coupling in mimo wireless systems: A rigorous network theory analysis *Wireless Communications, IEEE Trans.* **3** 1317–25
- [27] van Valkenburg M E and van Valkenburg M 1964 *Network Analysis* vol 3 (Upper Saddle River, NJ: Prentice-Hall)
- [28] Kuratsuji H, Botet R and Seto R 2007 Electromagnetic gyration: - hamiltonian dynamics of the Stokes parameters *Prog. Theor. Phys.* **117** 195–217
- [29] Engø K 2001 On the bch-formula in so (3) *BIT Numerical Mathematics* **41** 629–32
- [30] Hladik J 1999 *Spinors in Physics* (New York: Springer)